2019 Rock Dynamics Summit– Aydan et al. (eds)
© 2019 Taylor & Francis Group, London, ISBN 978-0-367-34783-3

Numerical simulation on progressive failure in rock slope using a 3D lattice spring model

Tsuyoshi Nishimura & Masanori Kohno
Tottori University, Tottori, Japan

ABSTRACT: In slope stability analyses, the failure surface is often assumed to be predefined as a persistent flat or circular concave plane and the slide resistance along the plane is evaluated. Though this procedure gives the safety factor based on the limit equilibrium theory, the existence of such plane is highly unlikely, and a complex interaction between pre-existing flaws, stress concentration and resulting crack generation, these are not modeled. The development of advanced numerical methods is the key issues of importance. This paper attempts to develop a numerical procedure providing means to analyze the kinetic failure process and the state of stability using a discrete approach. The ground is modeled with an assembly of mass points connected by a pair of springs, normal and tangential direction and the translational motion of each mass point is calculated by solving the equation of motion. The stress state is evaluated on each mass point.

1 INTRODUCTION

Slope instability occurs in many parts of urban and rural areas and causes damages to housing, roads, railways and other facilities. Slope engineering has always involved some form of risk management and this has led to the process of the identification and the characterization of the potential slope failure together with evaluation of their frequency of occurrence. An essential part of the hazard (slope failure) identification is the prediction in terms of the character of failure (type, volume), the post-failure motion (travel distance, velocity) and the state of activity (Fell, et al. 2008). The literatures of slope stability analysis using the limit equilibrium method (LEM) and the finite element method (FEM) were reviewed by Duncan (1996), and a number of valuable lessons concerning the advantages and limitations of the methods for use in engineering problems were presented. Jing and Hudson (2002) presented a review of the techniques, advances problems and future development directions in numerical modeling for rock mechanics and rock engineering. The expanded version of the brief review was presented by Jing (2003) and he has suggested that computer methods available can be still inadequate when facing the challenge of practical problems, especially when representation of rock fracture systems and fracture behavior are a pre-condition for successful modeling. Despite of all the advances in both continuum and discrete approaches, the development of advanced numerical methods is the key issues of importance. This paper attempts to develop a numerical procedure providing means to analyze the kinetic failure process and the state of stability as a function of a trial gravitational acceleration to a lattice spring model. This procedure is also able to explain a possible depth and volume of failure at the site.

Most rock slopes are inhomogeneous structures comprising anisotropic layers of rock characterized by different material properties, and they are often discontinuous because of jointing, bedding and fault. In rock slope stability analyses, the failure surface is often assumed to be predefined as a persistent plane or series of interconnected planes, where the planes are fitted to the surfaces based on the structural observation. Such assumptions are partly due to the constraints of the analytical technique employed (e.g. limit equilibrium method, the distinct element method, etc.) and can be valid in cases in which the response of single discontinuity or a small number of discontinuities is of critical importance on the stability. However, especially on a large scale slope, it is highly unlikely that such a system of fully persistent discontinuous planes exists a priori to form the failure surface. Instead, the persistence of the key discontinuities may be limited and a complex interaction between pre-existing flaws, stress concentration and resulting crack generation, is required to bring the slope to failure. In small engineered slopes, excavation gives significant changes in stress distribution in the slopes and may generate fully persistent planes keep propagating with stress redistribution. Larger natural rock slopes seldom experience such a disturbance and have stood in relatively stable features over the period of thousands of years. This does not imply that in natural rock slopes a system of discontinuities may not be interconnected developing the portion of where the failure surface will be formed. Strength degradation may occur in rock mass with time-dependent manner and drive the slope unstable state. Thus, rock slope instability problem requires the progressive failure modeling to drive the slope to catastrophic events.

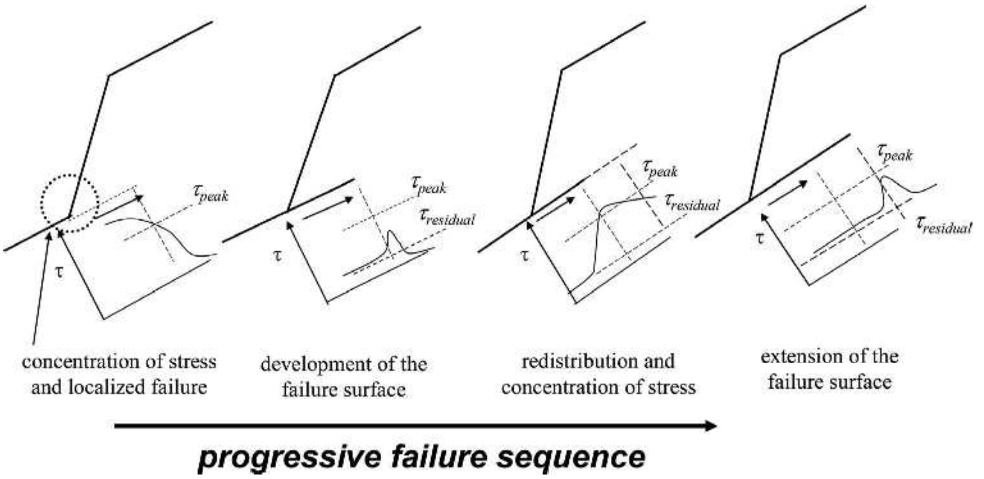

Figure 1. Failure surface initiation and its propagation (after Bjerrum (1967))

2 MODELING OF THE FAILURE SURFACE

Based on the coulomb shearing strength criterion, both the shearing resistance depending on the normal stress value (i.e. the frictional strength) and the cohesion of intact rock between discontinuous joints resist to shear failure. At the tip of the joints, stresses would increase and subsequent failure in rock would occur. Progressive failure in rock mass would involve the failure of intact rock as their strength is exceeded. There have been a number of investigations focused on the failure process of rock slope using the finite element method and the boundary element method.

Kaneko et al. (1997) used the displacement-discontinuity method (DDM) and fractures' principles to model the progressive development of shear crack in rock slope. In their analysis, rock material was assumed to be homogeneous and any pre-existing cracks were not considered. They compared the DDM results with the conventional limit equilibrium method (LEM) and discussed the allowable slope height under the given strength parameters and the slope angle. Eberhardt et al. (2004) discussed some aspects of the modeling of progressive failure surface development linking initiation and degradation to eventual catastrophic slope failure, using a hybrid method that combines both continuum and discontinuum numerical techniques to model fracture propagation. They concluded that the use of the hybrid modeling technique helped to provide important insight as to the underlying mechanism, focusing on the example of a rockslide in the Swiss Alps.

Developments in the field of rock slope analysis were reviewed by Stead et al. (2006). They have attempted to illustrate the wide range of tools available with particular emphasis on emerging powerful modeling of hybrid techniques that allow realistic simulation of rock slope failure. Generally, there are two choices of hybrid technique; technique of hybrid continuum-/discrete-element method and technique based on a discrete modeling. In the first choice, fracture plane is aligned in two ways shown in Figure 2.

1. a process known as intra-element fracturing where a series of new nodal points and elements are systematically created as shown Figure 2(b).
2. a process known as inter-element fracturing where a series of new nodal points are systematically created but no new element is generated as shown Figure 2(c). This process is usually preferred from the computational standpoint and the discrete fracture orientation is aligned with the best oriented element boundary attached to the node considered.

The presence of contact phenomena during post fracturing requires an effective contact simulation procedure. One fundamental advantage of the discrete modeling is that the phenomena can be incorporated into the method by the rigid body or the mass point contact with the spring-dashpot system. This method has been used to investigate a wide

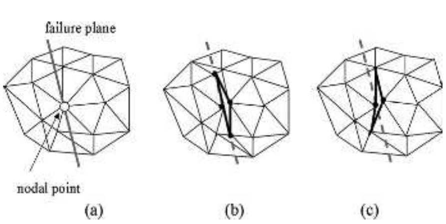

Figure 2. Modeling of crack generation: (a):element discritization and failure plane, (b)continuous discritization of elements along the direction of new cracks, (c) a priori placement of crack element along the possible direction of the crack propagation.

variety of rock failure mechanisms. In these analyses, cracks propagate with the path calculated by the failure criterion under the stress state. This paper presents a numerical trial to simulate the progressive development of failure surface in slope.

3 DISCRETE ELEMENT MODELING FOR ELASTICITY

The body to be analyzed is divided into small portions and is represented by a system of points linked together with the neighboring points. The particles and bonds form a network system representing the material. For this system, the equation of motion can be expressed as

$$\mathbf{m}\ddot{\mathbf{u}} + \mathbf{c}\dot{\mathbf{u}} + \mathbf{k}\mathbf{u} = \mathbf{f} \tag{1}$$

where $\mathbf{u}$ represents the vector of particle displacement, $\mathbf{k}$ is the stiffness, $\mathbf{m}$ is the mass matrix, $\mathbf{c}$ is the damping matrix and $\mathbf{f}$ is the vector of external force. Equation (1) is solved by using the explicit finite difference scheme.

$$\ddot{\mathbf{u}}_t = \frac{1}{\mathbf{m}}\left[\mathbf{f} - \mathbf{c}\dot{\mathbf{u}}_t - \mathbf{k}\mathbf{u}_t\right] \tag{2}$$

The displacement of particle at time t+Δt can be expressed as

$$\Delta\mathbf{u}_t = \Delta\mathbf{u}_{t-\Delta t} + \ddot{\mathbf{u}}_t \Delta t^2 \tag{3}$$

where $\Delta\mathbf{u}_t=\mathbf{u}_{t+\Delta t}-\mathbf{u}_t$. The new position of particle is also expressed as

$$\mathbf{u}_{t+\Delta t} = \mathbf{u}_t + \dot{\mathbf{u}}_t\Delta t + \ddot{\mathbf{u}}_t \Delta t^2/2 \tag{4}$$

The particle velocity at t is given by

$$\dot{\mathbf{u}}_t = \frac{\mathbf{u}_t - \mathbf{u}_{t-\Delta t}}{\Delta t} + \ddot{\mathbf{u}}_t \Delta t/2 \tag{5}$$

To keep the computation stable, the time step could be chosen as

$$\Delta t < \min\left(\frac{d_0}{c_\mathrm{p}}\right) \tag{6}$$

where d_0 is the contact length, that is the distance between particles, and c_p is the P-wave velocity. For static simulation, the equations of motion are damped to reach an equilibrium state under given boundary conditions as quickly as possible. In this modeling, the damping effect is incorporated as written in the following.

$$\ddot{\mathbf{u}}_t = \frac{1}{\mathbf{m}}\left(\sum \mathbf{f}_t - \mathrm{sgn}(\dot{\mathbf{u}}_{t-\Delta t})\cdot \alpha\left|\sum \mathbf{f}_t\right|\right) \tag{7}$$

where α is the damping constant which is independent of mechanical properties of the material.

We assume that the medium is loaded from zero condition to an initial condition defined by the strain e_{ij} and the stress σ_{ij}. For such a system, one can write the displacement for a particle (or element) p with position x_i as follows

$$u_i^\mathrm{p} = e_{ij} x_j^\mathrm{p} \tag{8}$$

where e_{ij} should be a symmetric tensor which is calculated by removing an asymmetric tensor from the displacement-gradient tensor. The rotation-related term is removed from the relative translational displacement between these two points, then this method ensures that the calculated strain is independent of rotational displacement (Nishimura, T. et. al. 2014).

The following contact law, which relates normal and shear forces $F_{(n)}$, $F_{(s)}$ to normal and shear relative displacements $U_{(n)}$, $U_{(s)}$ holds at the contact

$$F_{(\mathrm{n})} = k_\mathrm{n} U_{(\mathrm{n})},\ F_{(\mathrm{s})} = k_\mathrm{s} U_{(\mathrm{s})} \tag{9}$$

Let us assume that a contact m connects two particles p1 and p2, then the normal and shear relative displacements can be written as

$$U_{(\mathrm{n})}^m = \Delta u_i^m I_i^m \tag{10}$$

$$U_{(\mathrm{s})i}^m = \Delta u_i^m - U_{(\mathrm{n})}^m I_i^m \tag{11}$$

where the relative displacement at the contact Δu_i^m is given as

$$\Delta u_i^m = e_{ij}\left(x_j^{\mathrm{p}1} - x_j^{\mathrm{p}2}\right) = e_{ij} d_b^m I_j^m \tag{12}$$

where I_i^m is the normal unit vector. The total force f_i at contact m can be written as

$$\begin{aligned} f_i^m &= k_\mathrm{n}^m \Delta u_j^m I_j^m I_i^m + k_\mathrm{s}^m\left(\Delta u_i^m - \Delta u_j^m I_j^m I_i^m\right) \\ &= \left(k_\mathrm{n}^m - k_\mathrm{s}^m\right)\left(e_{kl} I_k^m I_l^m\right) I_i^m d_b^m + k_\mathrm{s}^m e_{ij} I_j^m d_b^m \end{aligned} \tag{13}$$

Notice that Einstein summation convention with dummy subscript i, j, k, l is used in the preceding equations. The total strain energy stored per unit volume is

$$\Pi = \frac{\Pi_b}{V} = \frac{1}{V}\sum_{m=1}^{N_c}\frac{1}{2}\left(e_{ij} d_b^m I_j^m f_j^m + e_{ji} d_b^m I_i^m f_i^m\right) \tag{14}$$

where N_c is the number of contacts inside the medium, V is the medium volume. The stress tensor of the continuum can be obtained through the classical elastic theory, and it can be written as (assuming symmetrical stress) (Walton, K. 1987, Richard, J. B. & Leo, R. 1988).

$$\sigma_{ij} = \frac{1}{2V}\sum_{m=1}^{N_c}\left(d_b^m I_i^m f_j^m + d_b^m I_j^m f_i^m\right) \tag{15}$$

From Equations (13) and (15), we end up with

$$\sigma_{ij} = \frac{1}{V}\sum_{m=1}^{N_c}\frac{1}{2}\Big(k_s^m e_{jl} I_l^m I_i^m d_b^{m2} + k_s^m e_{il} I_l^m I_j^m d_b^{m2} + \left(k_n^m - k_s^m\right) e_{kl} I_i^m I_j^m I_k^m I_l^m d_b^{m2}\Big) \quad (16)$$

The constitutive matrix C_{ijkl} in the classical elasticity theory is expressed as

$$\sigma_{ij} = C_{ijkl} e_{kl} \quad (17)$$

and finally, by substituting Equation (17) into Equation (16), C_{ijkl} can be given as

$$C_{ijkl} = \frac{1}{V}\sum_{m=1}^{N_c}\left(\frac{k_s^m d_b^{m2}}{4}\left(I_j^m I_k^m \delta_{il} + I_i^m I_k^m \delta_{jl} + I_j^m I_l^m \delta_{ik} + I_i^m I_l^m \delta_{jk}\right) + \left(k_n^m - k_s^m\right) d_b^{m2} I_i^m I_j^m I_k^m I_l^m\right) \quad (18)$$

where δ_{ij} is the Kronecker's delta. Then, the relationship the micro-mechanical parameters k_n, k_s and the macro material constants the Young' modulus E_0 and the Poisson's ratio v_0 can be obtained by comparing Equation (18) to the classical elastic matrix. As seen in this equation, the values of the stiffness are influenced by the normal unit vector, therefore, the lattice structure should be carefully modeled. A 18-bond cubic lattice geometry as shown in Figure 3 is prepared. The micro-mechanical parameters k_n, k_s are obtained by

$$k_n = \frac{E_0 d_0}{5\left(1-2v_0\right)} \quad (19)$$

$$k_s = \frac{\left(1-4v_0\right)E_0 d_0}{5\left(1+v_0\right)\left(1-2v_0\right)} \quad (20)$$

Equation (20) shows that the spring stiffness of negative occurs when v_0 is greater than 0.25. For this condition, we have failed to obtain the quasi-static state under a given static boundary condition and the model shows unstable behavior. Therefore, numerical results shown in this paper are carried out for $v_0<0.25$. This negative effect of the Poisson's ratio in such lattice modeling has also been reported (e.g. Zhao, G. F. Fang, J. & Zhao, J. 2011).

4 NUMERICAL SIMULATION ON PROGRESSIVE FAILURE IN SLOPE

Figure 3 shows the slope model which is formed by the discrete lattice spring model. The height of slope h is 100m and the bottom width w is 200m. Slope inclination is expressed with tanβ=2 (β=63.7°). The Young's modulus and the Poisson's ratio are set 1000MPa and 0.24 respectively. Figure 4 shows the results of τ_{xy} for g=9.8m/s^2 (1G) and the stress concentration is recognized around the slope toe. Then, the gravitational acceleration is assumed to increase as nG (n>1). This condition is to load the slope model and to simulate the progressive development of failure surface and slope instability. We have introduced the Mohr-coulomb failure criterion written as;

$$F = (\sigma_1 - \sigma_3) + (\sigma_1 + \sigma_3)\sin\phi - 2c\cos\phi \quad (21)$$

σ_1: the major principal stress, σ_3: the minor principal stress, c: cohesion, ϕ: frictional angle. When F=0 the stress state fulfills the failure criterion and F>0 represents by points outside the failure surface. Plastic strains may develop during increment from an initial state belonging to the yield surface (F=0). The plastic strain is governed by the plastic flow rule and then the corresponding stress increment to the elastic strain is evaluated so as to hold the stress state on/inside the yield surface. This procedure is the same to the ordinal numerical modeling of plasticity.

Figure 5 demonstrates the transition from stable slope conditions to those of shear failure by showing the evolution of failure points. The parameter related to the strength are set to c=35kPa, ϕ=50° and these values keep constant and no reduction is assumed during the loading. Though the assumptions are introduced, this numerical modeling can be used to examine the evolution of stresses strain and failure surface development within the rock slope. From

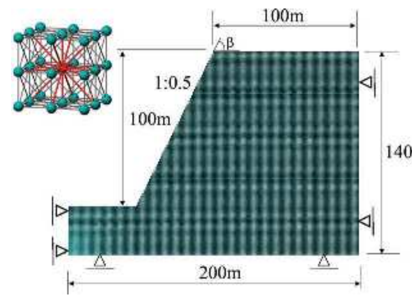

Figure 3. Rock slope model with constant inclination using the assembly of circular element.

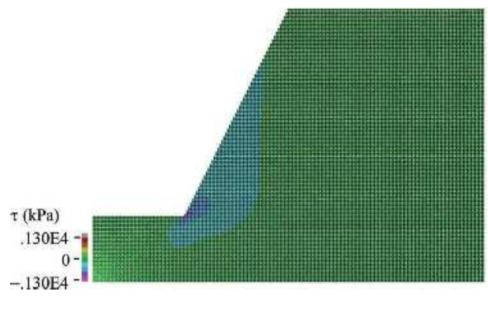

Figure 4. Distribution of τ_{xy}

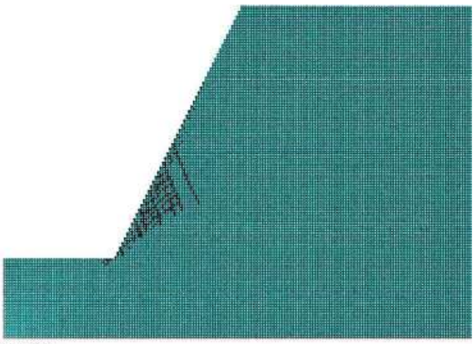

(a)1.8G

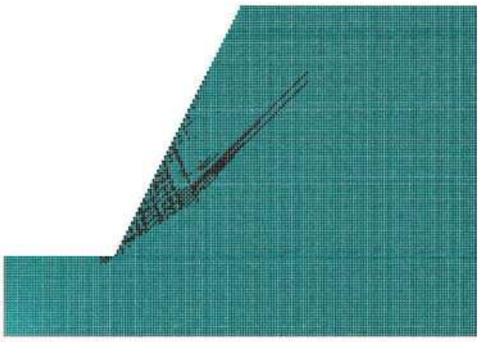

(b)2.0G

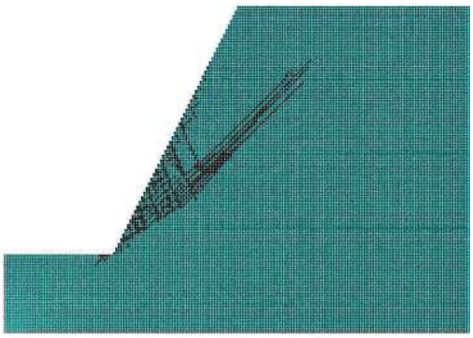

(c)2.2G

Figure 5. Progressive development of failure surface.

these figures, the shear-based Mohr-coulomb fracture surface has propagated from the toe of the slope model to the inner part. These figures also involve the progressive fracturing cross to the shear-based surface mentioned the above. To more closely examine these mechanisms for the development, it can be recognized that firstly the shear-based fracture surface has propagated from the toe of the slope and secondly the tensile crack propagate in the slide mass as illustrated in Figure 6. The failure criterion used in this simulation is set up to explain tensile failure without the inclusion of a predefined failure element and the stress state on the mass point calculated by Equation

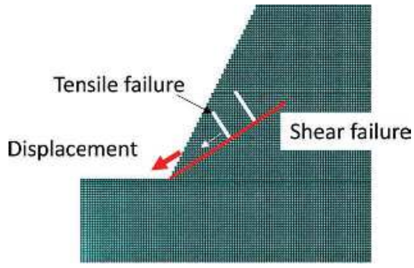

Figure 6. Development of shear surface and propagation of tensile damage upwards through slide mass, dividing the slide mass into blocks.

(15) and examined by Equation (21), the stress state is inside the failure criterion or outside including tensile fracturing. Results show that a zone of yield due to shear damage develops near the toe of slope and this development transforms into a tensile failure in the slide body. This transformation of failure continues through the body and divides the body into blocks. These progressive fracturing must lead the mass to collapse of the frontal region of the slope. This model results agree with the analysis by Eberhaldt (2004).

5 CONCLUSION

Various numerical methods (continuum and discontinuum methods, and hybrid methods which combine both continuum and discontinuum techniques to simulate fracturing process) have been applied to demonstrate the evolution of failure in rock slope. In this paper, a numerical modeling of progressive failure in rock mass using the discrete lattice spring model is introduced to simulate the rock slope failure. The modeling could give a possible failure volume of rock material based on the geometrical data and strength properties, such as cohesion and internal friction angle. No decisive statement about the effect of the mechanical parameters can be made because the analysis was performed under the limited input values. On going work should be done incorporating the effects of the macro parameters and the initial stress condition.

ACKNOWLEDGEMENT

This work is partly supported by Japanese Society for the Promotion of Sciences (JSPS), Grant-in-Aid for Science Research, No.17K06554.

REFERENCES

Bjerrum, L. 1967. Progressive failures in slopes of overconsolidated plastic clay and clay shales, *Journal of Soil Mechanics and Foundation Division, ASCE*, 93(SM), 1–49.

Duncun, J. M. 1996. State of the art: Limit equilibrium and finite element analysis of slopes. *Journal of Geotechnical Engineering, ASCE*, 122(7),577–596

Eberhardt, E., Stead, D. & Coggan, J. S. 2004. Numerical analysis of initiation and progressive failure in natural rock slopes - the 1991 Randa rockslide. *International Journal of Rock Mechanics and Mining sciences*, 41(1),69–87.

Fell, R., Corominas, J., Bonnard, C., Cascini, L., Leroi, E. & Savage, W. Z. 2008. Guideline for landslide susceptibility, hazard and risk zoning for land use planning, *Engineering Geology*, 102(3/4), 85–111.

Kaneko, K., Otani, J., Noguchi, Y. & Togashiki, N. 1997. Rock fracture mechanics analysis of slope failure. *Defomation and Progressive failure in Geomechanics*, Nagoya, Japan, 671–676.

Ling, L. & Hudson, J. A. 2002. Numerical methods in rock mechanics. *International Journal of Rock Mechanics and Mining sciences*, 39(4),409–427.

Ling, L. 2003. A review of techniques, advances and outstanding issues in numerical modelling for rock mechanics and rock engineering. *International Journal of Rock Mechanics and Mining sciences*, 40(3),283–353.

Nishimura, T., Fumimura, K., Kohno, M. & Mitsuhashi, D. 2016. 3D Distinct Element-Based Model for Deformation and Failure of Rock, *Proceedings of 2016 ISRM Interna-tional Symposium - 9th Asian Rock Mechanics Symposi-um*, PO4–P74.

Richard, J. B. & Leo, R. 1988. Note on a random isotropic granular material with negative Poisson's ratio, *International Journal of Engineering Science*, 26(4),373–383.

Stead, D., Eberhardt E. & Coggan, J. S. 2006. Developments in the characterization of complex rock slope deformation and failure using numerical modeling techniques, *Engineering Geology*, 83(1/3), 217–235.

Walton, K. 1987. The effective elastic moduli of a random packing of spheres, *Journal of the Mechanics and Physics of Solids*, 35(2),213–226.

Zhao, G. F., Fang, J. & Zhao, J. 2011, A 3D distinct lattice spring model for elasticity and dynamic failure, *International Journal for Numerical and Analytical Methods in Geomechanics*, 35(8),859–885.